

Bond Breaking, Electron Pushing, and Proton Pulling: Active and Passive Roles in the Interaction between Aqueous Ions and Water as Manifested in the O 1s Auger Decay

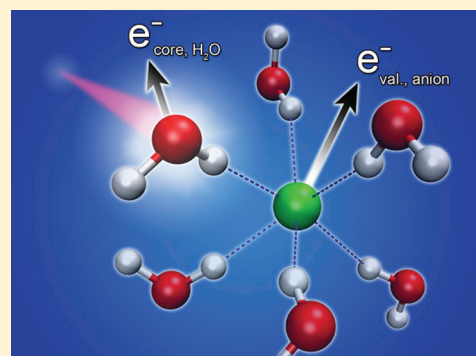
W. Pokapanich,^{*,†} N. Ottosson,[†] S. Svensson,[†] G. Öhrwall,[‡] B. Winter,^{*,§} and O. Björneholm^{*,†}

[†]Department of Physics and Astronomy, Uppsala University, Box 516, SE-751 20 Uppsala, Sweden

[‡]MAX-lab, Lund University, P.O. Box 118, SE-221 00 Lund, Sweden

[§]Helmholtz-Zentrum Berlin für Materialien und Energie, and BESSY, Albert-Einstein-Strasse 15, D-12489 Berlin, Germany

ABSTRACT: A core-ionized H₂O molecule in liquid water primarily relaxes through normal Auger decay, leading to a two-hole final state in which both valence holes are localized on the same water molecule. Electronic coupling to the environment, however, allows for alternative decays resembling Intermolecular Coulombic Decay (ICD), producing final states with one of the holes delocalized on a neighboring water molecule. Here we present an experimental study of such minority processes, which adds to our understanding of dynamic interactions of electronically excited H₂O molecules with their local surrounding in liquid water and aqueous solution. We show that the solvation of metal-halide salts considerably influences these minority decay channels from the water O 1s⁻¹ state. By breaking water–water bonds, both the metal cations and halide anions are found to reduce the decay into water–water delocalized states, thus having a “passive” effect on the Auger spectrum. The halide anions also play an “active” role by opening a new ICD-like decay pathway into water-halide delocalized states. The importance of this contribution increases from F⁻ to I⁻, which we suggest to be caused by a directional polarization of the halide anion toward the core-ionized H₂O⁺ cation in the intermediate state of the Auger process. This increases the electronic overlap between the two centers and makes delocalized decays more probable. We furthermore show that F⁻, the smallest and most strongly hydrated of the halides, plays an additional role as proton puller during the core-hole lifetime, resulting in proton dynamics on the low femtosecond time scale. Our results represent a step forward toward a better understanding of how aqueous solutions, when exposed to soft X-rays, channel excess energy. This has implications for several aspects of physical and radiation chemistry, as well as biology.



1. INTRODUCTION

Core ionization of a water molecule results in a highly localized and unstable (1s)⁻¹ cationic state that quickly relaxes through normal Auger decay in which one valence electron fills the core hole, while another valence electron is emitted. Depending on the chemical environment of the core-ionized molecule, different decay pathways are possible, as schematically shown in Figure 1. A free core-ionized H₂O molecule in the gas phase almost exclusively relaxes through normal Auger-electron decay (only ~1% decays by fluorescence), producing localized two-hole final states with the two valence vacancies residing on the same water molecule;^{1–3} we here denote such states as W^{v-2} . The situation is illustrated in branch ia in Figure 1.

If the core-ionized molecule is part of the hydrogen (H) bonding network of liquid water, this channel still dominates the O 1s decay spectrum (Figure 1ii, channel a), but new de-excitation pathways open up due to the efficient electronic coupling between the H-bonded neighboring water molecules. As illustrated in channel b of panel ii, the surrounding water enables Auger decays of Intermolecular Coulombic Decay (ICD) type,^{4,5} to delocalized $W^{v-1}W^{v-1}$ final states, in which the two final-state valence holes reside on different molecules.⁶ Due

to the increased spatial separation between the two holes, which reduces the Coulomb repulsion, these final states are lower in energy compared to the localized W^{v-2} states. Therefore, they give rise to higher kinetic energy (KE) features in the Auger electron spectrum, found exclusively in the condensed phase.

In the present work, we study how this branching of the O 1s Auger decays changes in the presence of inorganic salt ions in the solutions. Conceptually, the introduction of the solute allows for additional delocalized two-hole final states, with one valence hole residing on a solvated ion. Such $W^{v-1}A^{v-1}$ and $W^{v-1}C^{v-1}$ states, for anions (A) and cations (C), respectively, are reached via channel c as illustrated in panels iii and iv of Figure 1. To quantitatively assess the effects of solvated metal cations and halide anions on the processes shown in Figure 1, we have performed Auger electron spectroscopy (AES) studies of various aqueous solutions, chosen so that we can single out the respective effects of the anions and the cations. We find that cations primarily play a passive role by breaking water–water H-bonds,

Received: May 4, 2011

Revised: November 20, 2011

Published: November 22, 2011

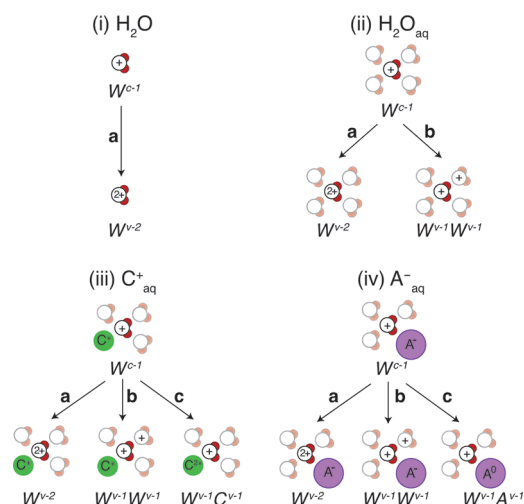


Figure 1. Illustration of different possible two-hole final states resulting from H_2O oxygen 1s Auger processes in the free water molecule (i), in pure liquid water (ii), and in aqueous salt solution; (iii) and (iv) describe the situation when a core-ionized water molecule resides in the first solvation shell of an anion and a cation, respectively.

which reduces the efficiency for forming $W^{V-1}W^{V-1}$ states. The comparison between the aqueous ammonium halides NH_4X ($\text{X} = \text{F}, \text{Cl}, \text{Br}, \text{I}$) however shows that halide anions play more active roles, both as providers of electrons to ICD-like Auger decay and as inducers of proton dynamics.

2. EXPERIMENTAL SECTION

All measurements were performed at the German synchrotron laboratory BESSY, Berlin, at the soft X-ray undulator beamline U41-PGM. The liquid O 1s Auger spectra were obtained from a 20 μm liquid jet, injected into a differentially pumped vacuum chamber. Electrons were detected by a hemispherical electron analyzer (Specs Leybold EA10), which was mounted at 90° relative to the polarization plane, perpendicular to the propagation of the liquid jet. Typical working pressures were in the 10^{-5} mbar range in the experimental chamber and in the low 10^{-7} mbar region in the electron analyzer. The temperature of all solutions was kept fixed at 4°C . Further details on the setup have been described elsewhere.^{7,8} Aqueous LiBr and MgBr_2 were prepared by dissolving high purity salts ($\geq 99.0\%$, Sigma-Aldrich) with highly deionized water to obtain aqueous solutions of 6 and 3 m , respectively. The concentration of bromide anions was hence identical (6 m) in both solutions. In addition, aqueous ammonium-halide solutions, NH_4F , NH_4Cl , NH_4Br , and NH_4I ($\geq 99.0\%$, Sigma-Aldrich), were prepared, each at 5 m concentration.

The O 1s Auger electrons from pure water and from the aqueous salt solutions were recorded with 650 eV photon energy, except for the aqueous iodide compounds (NH_4I), in which case the photon energy was 615 eV. At this energy, spectral overlap of the O 1s and I^- MNN Auger features is avoided. The iodide 3d thresholds lie at 624.2/635.7 eV binding energy (BE) for the 5/2 and 3/2 spin orbit components, respectively.⁹ Notice that all photon energies used are well above the oxygen K-edge absorption fine structure, thereby producing core-ionized states upon O 1s photoabsorption. The KE scale was calibrated using the H_2O gas-phase O 1s Auger lines, which were measured when the liquid

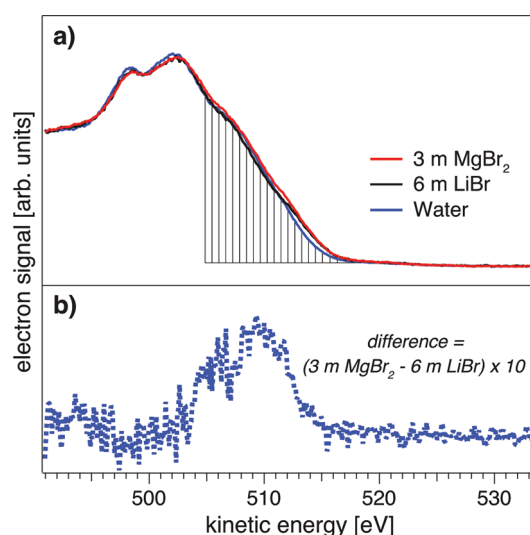


Figure 2. Top part shows oxygen 1s Auger-electron spectra from 3 m MgBr_2 (red) and 6 m LiBr (black) aqueous solutions and neat water (blue). The bottom trace is the difference between the two solution spectra, i.e., $\text{MgBr}_2 - \text{LiBr}$.

jet was displaced from its optimum position. The total experimental resolution for all Auger spectra was approximately 250 meV, i.e., much narrower than the natural line widths of the broad Auger structures.

3. RESULTS AND DISCUSSION

3.1. Li^+ and Mg^{2+} Cations Acting As Passive Bond Breakers. In the following, we will make a comparison between LiBr and MgBr_2 solutions of identical Br^- concentration to reveal the effect of the cations on the water O 1s decay. The simplest hypothesis is that the amount of cationic species added passively determines to which degree the O 1s decay of a core-ionized water molecule can couple to a neighboring water molecule to form delocalized $W^{V-1}W^{V-1}$ states, simply due to the reduced number of H_2O molecules which on average resides in the first hydration shell of a water molecule.

In the upper panel of Figure 2, we show the O 1s Auger spectra of neat water and aqueous solutions of 6 m LiBr and 3 m MgBr_2 . Their relative intensities are adjusted such that the spectra overlap at the high and low KE ends. For pure water, the region with $\text{KE} > 505$ eV (highlighted in the figure) exclusively contains contributions from delocalized $W^{V-1}W^{V-1}$ states produced via channel iib in Figure 1. Relaxation to localized W^{V-2} states via channel iia of Figure 1 contributes at $\text{KE} < 505$ eV. We find that the spectra of the LiBr and MgBr_2 solutions indeed overlap everywhere except in the 500–520 eV KE region.

To separate the effects induced by cations versus halide anions, the difference between the spectra of the 6 m LiBr and 3 m MgBr_2 solutions is displayed in the bottom panel of Figure 2. Note that these features must primarily be due to differences in the effects that the Li^+ and Mg^{2+} cations have on the water O 1s Auger decay. The broad structure in the difference spectrum around 500–520 eV KE is exactly in the region of the $W^{V-1}W^{V-1}$ states, produced in neat water (channel b of Figure 1ii). This means that in a solution of 6 m Li^+ cations there are fewer decays to delocalized $W^{V-1}W^{V-1}$ states than in a solution of 3 m Mg^{2+} cations. It is natural to rationalize this finding in terms of the relative density

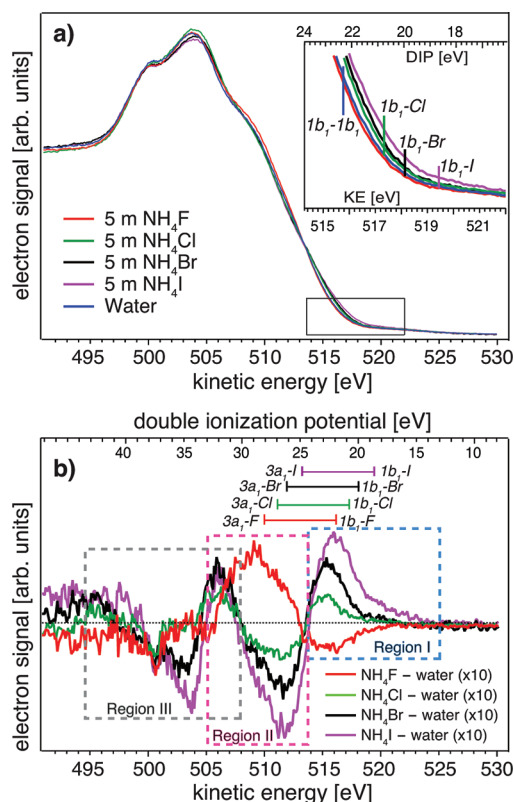


Figure 3. (a) Oxygen 1s Auger electron spectra from pure water (blue) and 5 *m* aqueous ammonium halide solutions: NH₄I (purple), NH₄Br (black), NH₄Cl (green), and NH₄F (red). The framed area is shown enlarged in the top-right inset, shown with both a kinetic energy and double ionization potential scale (for explanation of notations 1b₁-I, 1b₁-Br, 1b₁-Cl, 1b₁-F, and 1b₁-1b₁, see text). (b) Differential spectra, solution minus its referenced pure water, magnified ten times for better visibility. Note that the pure water spectrum in (a) is an example only. The dashed squares highlight the three different regions: 514–525 eV (I), 505–514 eV (II), and below 508 eV (III). The DIP energies, represented by the horizontal bars, show the lower and upper energetic bounds related to the 1b₁-X and 3a₁-X states of the respective solution, where X = I, Br, Cl, and F.

of water–water H-bonds in the two solutions, as this should correlate with the efficiency for forming $W^{v-1}W^{v-1}$ states. Even though Mg²⁺ has a larger fraction of water molecules in the first solvation shell than Li⁺ (approximately six vs four waters^{10–13}), the lower concentration of Mg²⁺ compared to Li⁺ (3 *m* vs 6 *m*) results in fewer water–water bonds being broken in the MgBr₂ solution, which explains the experimental observation. The additional channel iii_c, depicted in Figure 1, could however not be observed. We conclude that for the decay of the water O 1s core-hole in aqueous electrolytes metal cations have a passive influence by reducing the water–water coordination.

3.2. Halide Anions Acting as Electron Pushers and Proton Pullers. Having identified the main effects of the cations, we now turn our attention to the effects of anions on the O 1s core-hole decays of aqueous solutions. We do this by comparing Auger spectra of solutions of aqueous ammonium halides NH₄X (X = F, Cl, Br, I) at 5 *m* concentration (see Figure 3a). Intensities were normalized to yield the same total integrated area for each spectrum. Although the salt concentration is considerable, the solution Auger spectra are not very different from the one of neat

water. Most noticeable are the small and systematic intensity changes at the high-KE tail, near 514–525 eV. This region is magnified in the inset of Figure 3a. In addition, in Figure 3b, we display differential spectra (solution minus conjunctionally recorded water spectra) for each salt.¹⁴ Note that inequalities between the respective differential spectra must primarily be due to the nature of the respective halide anion since the concentration of ammonium cations is the same in all cases. Given the aforementioned intensity normalization, the variations in the difference spectra of Figure 3b reflect anion-induced intensity redistributions between the various Auger channels.

The first effect of the halide ions on the H₂O Auger decay which we consider is the decrease of the $W^{v-1}W^{v-1}$ states observed for the NH₄I, NH₄Br, and NH₄Cl cases, which lie in the KE range labeled as region II in Figure 3b. As was discussed in the previous section, the efficiency for this channel depends on the density of water–water H-bonds in the solution. At the current experimental conditions, where halide ions are seen to clearly affect the spectra, almost half of the water–water hydrogen bonds are broken in favor of ion–water bonds. However, if the reduced water–water coordination in the ionic solutions relative to pure water would be the only ion-induced effect on the O 1s Auger decay, we would expect the diminished number of decays to delocalized $W^{v-1}W^{v-1}$ states to be exactly compensated for by an increased number of decays to localized W^{v-2} states. This would be manifested as a mere redistribution of spectral intensity from region II to region III in Figure 3b. Clearly, this is not observed, and in the case of I[−], Br[−], and Cl[−], the reduction in region II rather seems compensated for by spectral intensity at higher kinetic energies, denoted as region I in Figure 3b. We note that the spectra of aqueous NH₄F, albeit different from the other solutions, cannot be described so simplistically, though. The model of anions merely playing a passive role in the O 1s Auger decay by breaking water–water bonds, which indeed could account for the behavior of cations, is hence insufficient to explain the anionic-specific features observed in the differential spectra of Figure 3b, suggesting that the halides are more actively involved in the water O 1s Auger decay.

We now turn to the 514–525 eV high-KE region I, as indicated in Figure 3b. If the BE of a given halide anion A[−] in water is lower than that of the HOMO 1b₁ BE of water, the energy of the lowest delocalized $W^{v-1}A^{v-1}$ final state will also be lower than for the $W^{v-1}W^{v-1}$ state. This is the case for aqueous Cl[−], Br[−], and I[−], with BEs of 7.3/7.7 eV for I[−] 5p_{3/2,1/2}, 8.8 eV for Br[−] 4p, and 9.6 eV for Cl[−] 3p,¹⁵ whereas the 1b₁ BE of water is 11.16 eV.¹⁶ We therefore assign positive intensities in region I of the difference spectra of Figure 3b to the formation of delocalized $W^{v-1}A^{v-1}$ final states produced via channel ivc of Figure 1. The observed energy shifts from Cl[−] over Br[−] to I[−] are indeed consistent with the decreasing BEs in the halide series. Using the above-mentioned BEs, we have calculated double ionization potentials (DIPs) for various $W^{v-1}W^{v-1}$ and $W^{v-1}A^{v-1}$ states and show the DIP energy scale on the upper axis in the inset of Figure 3a. For multiply ionized systems, one has to take into account the Coulomb repulsion between the two final state holes, which will depend on the distance of the two positive charges and on the degree of electronic screening in the ionized system. For $W^{v-1}A^{v-1}$ states, however, no Coulomb repulsion term is needed since the initially negative halide ions become neutral upon single valence ionization (electron detachment). In the following we use the notation 1b₁-I, 1b₁-Br, and 1b₁-Cl to denote the final states with a 1b₁ hole on the H₂O molecule and

one hole on the respective HOMO levels of the halides. Note that a Coulomb repulsion term in principle should be included for $W^{v-1}W^{v-1}$ states, such as the $1b_1-1b_1$ state, where both sites will be cationic in the final state. It has, however, previously been shown that this correction to the DIP is very small due to the efficient screening of the aqueous media,⁶ and it is therefore left out in the current analysis.

The DIP energies of the $1b_1-I$, $1b_1-Br$, $1b_1-Cl$, and $1b_1-1b_1$ states are at 18.7, 20.0, 20.8, and 22.3 eV, respectively, as shown in the inset of Figure 3a. Furthermore, since the final states may involve a hole from the manifold of water states ($1b_1$ to $2a_1$), the DIP energies water- X ($X = I, Br, Cl$) will then lie in the approximate ranges 19–25, 20–26, and 21–27 eV, respectively. These values reasonably well agree with the experimental observations and further strengthen the assignment that positive contributions to the difference spectra in region I of Figure 3b for the I^- , Br^- , and Cl^- cases indeed originate from water-halide delocalized final states, i.e., from channel c in panel iv of Figure 1. For F^- , the 2p BE has not yet been exactly determined by experiment, but it is estimated to be ~ 1 eV higher than for Cl^- .¹⁵ Hence, the $W^{v-1}F^{v-1}$ states would also appear in region I. The F^- difference spectrum, however, exhibits a decrease there. As the regions of $W^{v-1}W^{v-1}$ and $W^{v-1}A^{v-1}$ partially overlap, this suggests that any signal increase associated with delocalized $W^{v-1}F^{v-1}$ states will be smaller than the decrease caused by the reduction of delocalized $W^{v-1}W^{v-1}$ states.

As is evident from Figure 3b, the intensity of region I varies in the halide series, going from negative for F^- to increasingly positive with increasing halide size. What is the mechanism behind this behavior? One property that varies in the halide series is the hydration strength: weaker hydration of the larger halides results from the larger surface area over which the negative charge will be distributed, which leads to weaker interactions with water molecules in the first hydration shell. Beyond decreasing the ion–water distance, it has recently become clear that the ground-state charge transfer between the anion and the solvent also increases with decreasing halide size.^{17–19} Since it is reasonable to expect that the efficiency for forming delocalized two-hole states should increase with the charge transfer between the two centers, channel ivc could be expected to gradually become weaker going from F^- to I^- . This is however opposite to what is experimentally observed. We instead attribute the increase from F^- to I^- to the increased polarizability of the larger halides and its consequences in the intermediate state of the Auger decay. The core-ionized water molecule sitting in the first solvation shell of a polarizable negative halide will “pull” electron density from the anion toward the positive water molecular ion, thus increasing the probability for the halide electrons to participate in the decay process and produce delocalized $W^{v-1}A^{v-1}$ states (channel ivc). Another contributing factor is the decrease of the energy gain of the $W^{v-1}A^{v-1}$ states as compared to the $W^{v-1}W^{v-1}$ states with decreasing halide size, even becoming negative for F^- .

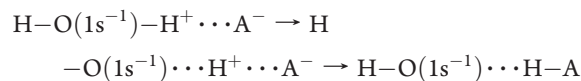
We now turn to the region below 508 eV KE (region III), in which the difference spectra for Cl^- , Br^- , and I^- exhibit an oscillation between positive and negative intensity, crossing zero at ~ 505 eV. Such an oscillation would result if the transitions to the localized W^{v-2} states, peaking at ~ 504 eV for pure water, were shifted toward higher KE for the Cl^- , Br^- , and I^- aqueous solutions. This means that for the water molecules in the first solvation shell of Cl^- , Br^- , and I^- ions the localized states would be shifted toward lower BE than for pure water. This can be understood as due to a combined effect of the structure in the

first solvation shell being more compact than in neat water, increasing screening, and a direct electrostatic potential caused by the close-by negative halide ion. Judging from the spectral profile of the decay to the W^{v-2} states,⁶ the shift of the transition to the W^{v-2} states between pure water and partially halide-coordinated water required to produce the observed oscillation is on the order of ~ 0.3 eV. The corresponding shift of singly charged states, such as the core-ionized final state, would be one-third of this value, i.e., ~ 0.1 eV. As far as we know, no such shift has been reported for halide-coordinated water molecules, but any component with such a shift could well be hidden in the inherently broad water O 1s peak of water and aqueous solutions.

The above arguments do not seem to apply for F^- ions, for which pronounced positive intensity in the 505–514 eV KE (region II) is observed. If we were to apply the analogous reasoning as for the Cl^- , Br^- , and I^- ions, a shift of the transitions to the W^{v-2} states with ~ 5 eV, corresponding to a water O $1s^{-1}$ shift of ~ 1.7 eV, would be implied. Such a large shift would however be easily identified in X-ray photoelectron spectroscopy but has not been observed. The mechanism explaining the Cl^- , Br^- , and I^- behavior can thus be ruled out for F^- . In search of another mechanism, we turn to look closer at the situation immediately after the core ionization of the water molecule. Core-ionized O $1s^{-1}$ is a bound state for free gas-phase water molecules, whereas it is dissociative for H-bonded ice and liquid water along one of the intramolecular O–H bonds.^{20–22} For water molecules situated in the first solvation shell of a halide A^- anion, one of the intramolecular O–H bonds points with the partially positive H toward the negatively charged halide A^- . This attraction will accelerate the O^*-H dissociation process by a Coulomb attraction between the positive proton and the negative halide A^- anion. The above arguments can be expressed in a chemically more intuitive form by use of the Z+1 (or equivalent core) approximation, according to which the valence electronic structure, and therefore the chemical properties, of a core-excited atom can be described as that of the following element in the periodic table.²³ The core-ionized $H_2O(1s^{-1})^+$ species can thus be approximated as H_2F^+ , and the local system immediately after core ionization can be described as a H_2F^+ ionic radical close to a halide A^- anion. This is not a stable arrangement, and the system will evolve toward two neutral molecules by proton transfer, as schematically described by the “reaction formula”, in which $O(1s^{-1})$ has been replaced by F



If we do not use the Z+1 approximation, this looks like



When interpreting Auger spectra, which reflect parallel ultrafast relaxation processes²⁴ (the O $1s^{-1}$ core hole lifetime is ~ 3.6 fs^{25,26}), we also need to consider spectral contributions from decays into intermediate species, ranging from $H_2O(1s^{-1})^+$ to $HO(1s^{-1})$. The Auger decay of free $HO(1s^{-1})$ has been studied both experimentally and theoretically since $HO(1s^{-1})$ is produced in the ultrafast dissociation of neutral core-excited free H_2O .^{27–29} To compare with the present experiment, the transition energies of free $HO(1s^{-1})$ have to be corrected for the effects of solvation. The energy of the neutral initial state, $HO(1s^{-1})$, is lowered by the solvation, but this solvation energy is 1 order of magnitude smaller than the solvation energy of the

charged final states of $(\text{HO}^{v-1})^+$. Neglecting the finer details, we use the shift observed for water, 1.75 eV,³⁰ when going from neutral H_2O to singly charged H_2O^+ , to approximate the solvation shift for transitions from $\text{HO}(1s^{-1})$ to $(\text{HO}^{v-1})^+$. Among the strong paths in the Auger decay of $\text{HO}(1s^{-1})$, the one with the highest KE then should be at ~ 512.25 eV, based on the values reported by Hjelte et al.²⁷

For the above-described nuclear dynamics induced by the core ionization of H_2O containing a halide anion in the first solvation shell, there will thus be positive contributions to the difference spectrum ranging from ~ 505 eV, for decays into intact $\text{H}_2\text{O}(1s^{-1})^+$, to ~ 512 eV, for decays into fully dissociated $\text{HO}(1s^{-1})$. This is consistent with the region of pronounced positive intensity observed for the F^- case in region II.

On a qualitative level, all of the above arguments for the proton dynamics in the intermediate $\text{O } 1s^{-1}$ core-hole state are also valid for the other investigated halides, Cl^- , Br^- , and I^- . For these three anions, however, the difference spectra of Figure 3 do not indicate that the effect is of large enough magnitude. To understand why this effect appears to only be really important for F^- , we have to invoke more quantitative arguments, considering both the initial and the core-ionized intermediate states.

Starting with the initial state effects, we note that F^- is the smallest of the halide ions. As a result, the dipolar water molecules can approach closer without experiencing Pauli repulsion and thus experience a stronger attracting electric field. On the basis of neutron diffraction, the bonding distance $\text{H}_2\text{O} \cdots \text{F}^-$ (2.54 Å) is considerably smaller than that for other halide ions ($\text{H}_2\text{O} \cdots \text{Cl}^-$, $\cdots \text{Br}^-$, and $\cdots \text{I}^-$ are 3.14, 3.32, and 3.63 Å, respectively³¹). The water molecule responds to the electric field of the ion by becoming polarized, shifting electron density away from the H–O bond oriented toward the negative ion. This destabilizes and elongates the intramolecular H–O bond, and again the effect is strongest for F^- . Having dealt with the initial state effects, we proceed to effects in the core-ionized intermediate state. The core-ionized water molecule is internally dissociative along one of the intramolecular O–H bonds. As detailed above, there will be an additional dissociative force for the proton in the H–O bond oriented toward the negative ion due to the Coulomb attraction from the negative ion. The attractive force is inversely proportional to the square of the ion–proton distance, again making the effect strongest for F^- . There are thus several effects that all should make the proposed proton dynamics most important for F^- . It should also be noted that even for F^- Auger decays involving proton dynamics is not a major process. It may be that it only occurs under favorable circumstances, for instance when thermal fluctuations in the water–ion distance and the water intramolecular vibrations happen to combine with the core ionization to give the proton maximum velocity toward the halide ion.

The core-hole Auger decays resulting in the here observed delocalized two-hole final states, both $W^{v-1}W^{v-1}$ and $W^{v-1}A^{v-1}$, have similarities to the ICD process, recently observed upon inner-valence ionization of liquid water clusters.³² For both the core and inner-valence cases, a hole localized on one water molecule decays in a process creating a hole on the initially ionized molecule and a neighboring molecule. A crucial difference between the two cases is that for inner-valence holes ICD is the only possible nonradiative decay process, thus only competing with the very slow radiative decay and proton transfer reactions,^{33,34} whereas for core-holes, normal localized Auger decay, resulting in W^{v-2} final states, strongly competes with the delocalized ICD-like decays. As for the actual physical mechanism of decay to

delocalized final states, we do not, however, see any fundamental difference between the inner-valence and core cases.

4. CONCLUSIONS

Using Auger electron spectroscopy, we have investigated how a core-ionized H_2O molecule in aqueous solution dissipates its excess electronic energy. It is found that the probability of different decay channels can be considerably altered when some of the first-shell water molecules are substituted by alkali cations or halide anions. Both metal cations and halide anions are seen to have primarily a passive effect on the O $1s$ core-hole decays by reducing the number of ICD-like decays to delocalized $W^{v-1}W^{v-1}$ states due to H_2O – H_2O hydrogen bonds being replaced by H_2O –ion bonds. The halide anions also play electronically more active roles. The larger halides Cl^- , Br^- , and I^- participate in ICD-like decays to delocalized $W^{v-1}A^{v-1}$ states. On a qualitative level, the underlying mechanism is the "pulling" of halide charge density toward the core-ionized water molecule, and consequently the efficiency of this decay channel increases with the polarizability of the halide anion. For F^- , which has the smallest polarizability of the halides, this ICD-like decay channel does not seem to be important. Due to its small size, and resulting strong hydration, F^- instead appears to induce proton dynamics in the O $1s$ core-hole state, pulling the nearest proton of the core-ionized water molecule toward itself and away from the remaining core-excited OH species.

As a final note, we want to point out that the presented results might be of some importance for better understanding the dynamics of de-excitation and formation pathways for ionized species and radicals in living cells when exposed to ionizing radiation. The present work thus represents a small step forward in the ambitious program of unraveling the mechanistic details of radiation-induced damage in biological tissue, e.g., upon radiotherapy.^{35–39}

AUTHOR INFORMATION

Corresponding Author

*E-mail: wandared.pokapanich@gmail.com; bernd.winter@helmholtz-berlin.de; olle.bjorneholm@fysik.uu.se.

ACKNOWLEDGMENT

The Royal Thai Government and Nakhon Phanom University are gratefully acknowledged for the graduate fellowship of W. Pokapanich. This work has been financially supported by the Swedish Research Council (VR), the Göran Gustafsson foundation, the Knut and Alice Wallenberg foundation, and Carl Tryggers Foundation. Additional support from the Deutsche Forschungsgemeinschaft (Project WI 1327/3-1) is gratefully acknowledged. We also thank BESSY staff for their helpful assistance during the experiments.

REFERENCES

- (1) Ågren, H.; Svensson, S.; Wahlgren, U. I. *Chem. Phys. Lett.* **1975**, 35, 336.
- (2) Siegbahn, H.; Asplund, L.; Kelfve, P. *Chem. Phys. Lett.* **1975**, 35, 330.
- (3) Caravetta, V.; Ågren, H. *Phys. Rev. A* **1987**, 35, 1022.
- (4) Cederbaum, L. S.; Zobeley, J.; Tarantelli, F. *Phys. Rev. Lett.* **1997**, 79, 4778.
- (5) Hergenroth, U. J. *Electron Spectrosc. Relat. Phenom.* **2011**, 184, 78.

- (6) Öhrwall, G.; et al. *J. Chem. Phys.* **2005**, *123*, 054310.
- (7) Winter, B.; Faubel, M. *Chem. Rev.* **2006**, *106*, 1176–1211.
- (8) Winter, B. *Nucl. Instrum. Methods Phys. Res., Sect. A* **2009**, *601*, 139–150.
- (9) Ottosson, N.; Faubel, M.; Bradforth, S. E.; Jungwirth, P.; Winter, B. *J. Electron Spectrosc. Relat. Phenom.* **2010**, *177*, 60.
- (10) Marcus, Y. *Chem. Rev.* **2009**, *109*, 1346.
- (11) Kristiansson, O.; Eriksson, A.; Lindgren, J. *Acta Chem. Scand.* **1984**, Ser. A 38a, 609.
- (12) Neilson, G. W. *Pure Appl. Chem.* **1988**, *60*, 1797–1806.
- (13) Newsome, J. R.; Neilson, G. W.; Enderby, J. E. *J. Phys. C: Solid State Phys.* **1980**, *13*, L923.
- (14) The differential spectra were made by subtraction of a solution spectrum and a water spectrum recorded immediately after each other. This means that different water spectra were used for different solution spectra. The separately recorded water spectra are very similar but not completely identical. The small differences are presumably due to minor differences in experimental alignment leading to somewhat different sensitivities to inelastically scattered background electrons. By using solution and water spectra recorded immediately after each other without any realignment in between, we avoid these problems. We also note that we have reproduced the results at several separate occasions and also for other salts.
- (15) Winter, B.; Weber, R.; Hertel, I. V.; Faubel, M.; Jungwirth, P.; Brown, E. C.; Bradforth, S. E. *J. Am. Chem. Soc.* **2005**, *127*, 7203–7214.
- (16) Weber, R.; Winter, B.; Schmidt, P. M.; Widdra, W.; Hertel, I. V.; Dittmar, M.; Faubel, M. *J. Phys. Chem B* **2004**, *108*, 4729.
- (17) Thompson, W. H.; Hynes, J. T. *J. Am. Chem. Soc.* **2000**, *122*, 6278–6286.
- (18) Mo, Y.; Gao, J. *J. Am. Chem. Soc.* **2006**, *110* (7), 2976–2980.
- (19) Robertson, W. H.; Johnson, M. A. *Annu. Rev. Phys. Chem.* **2003**, *54*, 173.
- (20) Brena, B.; Nordlund, D.; Odelius, M.; Ogasawara, H.; Nilsson, A.; Pettersson, L. G. M. *Phys. Rev. Lett.* **2004**, *93*, 148302.
- (21) Stia, C. R.; Gaigeot, M.-P.; Vuilleumier, R.; Fojón, O. A.; du Penhoat, M.-A. H.; Politis, M.-F. *Eur. Phys. J. D* **2010**, *60*, 77.
- (22) Odelius, M.; Ogasawara, H.; Nordlund, D.; Fuchs, O.; Weinhardt, L.; Maier, F.; Umbach, E.; Heske, C.; Zubavichus, Y.; Grunze, M.; Denlinger, J. D.; Pettersson, L. G. M.; Nilsson, A. *Phys. Rev. Lett.* **2005**, *94*, 227401.
- (23) Hüfner, S. *Photoelectron spectroscopy*; Springer Verlag: Berlin-GERMANY, 1995.
- (24) Björneholm, O.; Nilsson, A.; Sandell, A.; Hernnäs, B.; Mårtensson, N. *Phys. Rev. Lett.* **1992**, *68*, 1892.
- (25) Björneholm, O.; Sundin, S.; Svensson, S.; Marinho, R. R. T.; de Brito, A. N.; Gel'mukhanov, F.; Ågren, H. *Phys. Rev. Lett.* **1997**, *79*, 3150.
- (26) Neeb, M.; Rubensson, J. E.; Biermann, M.; Eberhardt, W. *J. Electron Spectrosc. Relat. Phenom.* **1994**, *67*, 261.
- (27) Hjelte, I.; Piancastelli, M. N.; Fink, R. F.; Björneholm, O.; Bässler, M.; Feifel, R.; Giertz, A.; Wang, H.; Wiesner, K.; Ausmees, A.; Miron, C.; Sorensen, S. L.; Svensson, S. *Chem. Phys. Lett.* **2001**, *334*, 151–158.
- (28) de Brito, A. N.; Feifel, R.; Mocellin, A.; Machado, A. B.; Sundin, S.; Hjelte, I.; Sorensen, S. L.; Björneholm, O. *Chem. Phys. Lett.* **1999**, *309*, 377.
- (29) Takahashia, O.; Odelius, M.; Nordlund, D.; Nilsson, A.; Bluhm, H.; Pettersson, L. G. M. *J. Chem. Phys.* **2006**, *124*, 064307.
- (30) Winter, B.; Aziz, E. F.; Hergenhahn, U.; Faubel, M.; Hertel, I. V. *J. Chem. Phys.* **2007**, *126*, 124504.
- (31) Soper, A. K.; Weckström, K. *Biophys. Chem.* **2006**, *124*, 180.
- (32) Mucke, M.; Braune, M.; Barth, S.; Förstel, M.; Lischke, T.; Ulrich, V.; Arion, T.; Becker, U.; Bradshaw, A.; Hergenhahn, U. *Nature Phys.* **2010**, *6*, 143.
- (33) Jahnke, T.; et al. *Nature Phys.* **2010**, *6*, 139.
- (34) Vendrell, O.; Stoychev, S. D.; Cederbaum, L. S. *ChemPhysChem* **2010**, *11*, 1006.
- (35) May, C. J.; Canavan, H. E.; Castner, D. *Anal. Chem.* **2004**, *76*, 1114.
- (36) Zubavichus, Y.; Fuchs, O.; Weinhardt, I.; Heske, C.; Umbach, E.; Denlinger, J. D.; Grunze, M. *Radiat. Res.* **2004**, *161*, 346.
- (37) Cai, Z.; Cloutier, P.; Hunting, D.; Sanche, L. *Radiat. Res.* **2006**, *165*, 365.
- (38) Ptasinska, S.; Stypczynska, A.; Nixon, T.; Mason, N. J.; Klyachko, D. V.; Sanche, L. *J. Chem. Phys.* **2008**, *129* (6), 129–134.
- (39) Stranden, E. *Pys. Med. Biol* **1977**, *22*, 348–352.